

## Features of DIRAC-99 T2 trigger data

M. V. Gallas<sup>b,†</sup>, C. Santamarina<sup>‡</sup>

<sup>b</sup> CERN; <sup>‡</sup> Universidade de Santiago de Compostela

### Abstract

The features of different DIRAC T2 trigger modes are shown in terms of the minimum relative distance between hits of all possible pairs. The behaviour of T2 electronics was simulated, using as input the recorded data from DE/DX and SFD detectors, to better understand the experimental data and to make predictions on some proposed improvements. The implications on the  $A_{2\pi}$ -detection were also studied through  $Q_x$  good-pair events distribution for different trigger-modes.

## 1 Introduction

As it is well known, the aim of DIRAC T2 trigger is to select the events with at least one pair of charged particles with relative x-distance less than 9 mm, using for that the SFD and DE/DX information. The level-2 trigger signal was, during 99-run III period and almost all 99-run II period, an OR of the following T2 trigger-modes:

- MODE I.- a pure DE/DX mode looking for double ionization hits in both planes of DE/DX detector:  $(A_i^{**} B_i^{**})$  OR  $(A_{i+1}^{**} B_{i+1}^{**})$ .
- MODE II.- combines the single adjacent DE/DX information with a veto(9-13) mm from SFD detector for selection of events with two minimum ionizing particles in two adjacent slabs of DE/DX detector:  $(A_i^* A_{i+1}^* \text{ OR } B_i^* B_{i+1}^*) \times \text{SFDveto}(9-13\text{mm})$ . The SFDveto(9-13mm) in x and y coordinates was removed in all T2 modes since run 164 (07/14/99).
- MODE III.- a pure SFD mode looking for events with at least a pair with relative distance < 9 mm.

The study of these modes takes as a data sample mainly the run 1036. This was collected on October the 4 th with  $T1_{\pi^+\pi^-}$  *coplanarity* trigger, Ni target, proton beam intensity  $6 \cdot 10^{10} p/spill$  and with  $\sim 400$  kevents size. Because differences were found between run II and run III periods, part of the analysis is also presented for the run 718 taken in run II period, August the 3 rd. This run was collected also with  $T1_{\pi^+\pi^-}$  *coplanarity* trigger, Ni target, proton beam intensity  $3 \cdot 10^{10} p/spill$  and with  $\sim 300$  kevents size. The data was processed through the ARIANE offline reconstruction program for data decoding and momentum analysis.

Due to the fact that T2 trigger is the OR of three modes, seven possible combinations are allowed and will be labeled by assignment of 1 to MODE-I, 2 to MODE-II and 4 to MODE-III. So all the possible combinations will appear in terms of these numbers and

their sums as shown in table 1 (an underlying binary representation is present). In this note they will be called T2-types.

	type 1	type 2	type 3	type 4	type 5	type 6	type 7
MODE I	yes	no	yes	no	yes	no	yes
MODE II	no	yes	yes	no	no	yes	yes
MODE III	no	no	no	yes	yes	yes	yes

Table 1: Correspondence between T2 modes and all their possible combinations, T2-types.

The initial point of this note will be figure 1 in which the proportion of each of these T2-types is shown with respect to the number of T1 triggers. To understand these proportions and the nature of each type itself should be the result of this study. The high proportion of type-1 and type-4 in relation to types-5,6,7 was not expected and could be an indication that something is not working properly. Types 1 and 4 mean that T2 trigger decision was taken only with one of the two detectors involved in upstream trigger. This could be due to events outside of the combined two detectors acceptance or to detectors or trigger inefficiencies.

As it was said, the aim of the upstream trigger is to select events with at least one pair of hits with  $x$  relative distance  $< 9\text{ mm}$ . So, we have analyzed the minimum relative distance per event in order to show the performance of all T2-modes. The following section presents these studies from the point of view of pure experimental data, expected behaviour by simulation of trigger electronics, and consideration of the possible implications in the  $A_{2\pi}$  detection by the analysis of  $Q_x$  distributions.

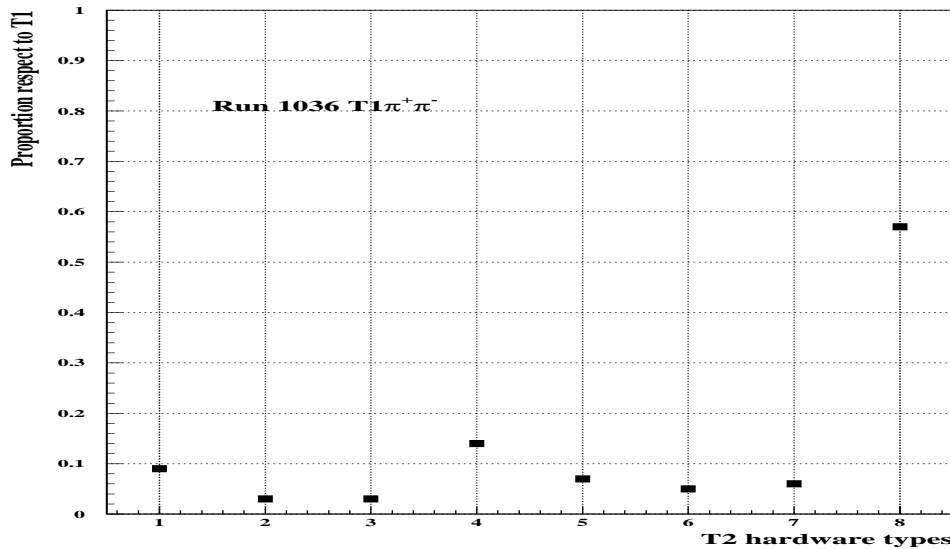


Figure 1: Rates of different T2-types with respect to the initial T1 triggers. The bin number 8 (the "0" of binary representation) means the proportion of T1 triggers without T2-marks.

## 2 T2-modes and T2-types behaviour

### 2.1 SFD-X minimum distance, experimental data

For each T1 trigger, the minimum distance between SFD hits in all possible pair combinations was calculated<sup>1</sup> and compared with the same quantity for all the T2 trigger types marked events. The ratio between these numbers is shown in figures 2 and 3. Figure 2 shows an efficiency<sup>2</sup> of  $\sim 70\%$  for the whole T2 trigger logic in region  $< 9\text{ mm}$  ( $= 20\text{ fibers}$ ) as well as a very poor efficiency ( $< 3\%$ ) for the types-1,2,3 in the same region. We have to remark the important statistics of type-1 at large distances, probably due to a low double ionization threshold. It is also important to note that the enhancement of fiber minimum distance for types 2 and 3 in the interval from 21 to 25 which is the working space of the not applied SFDveto(9-13mm).

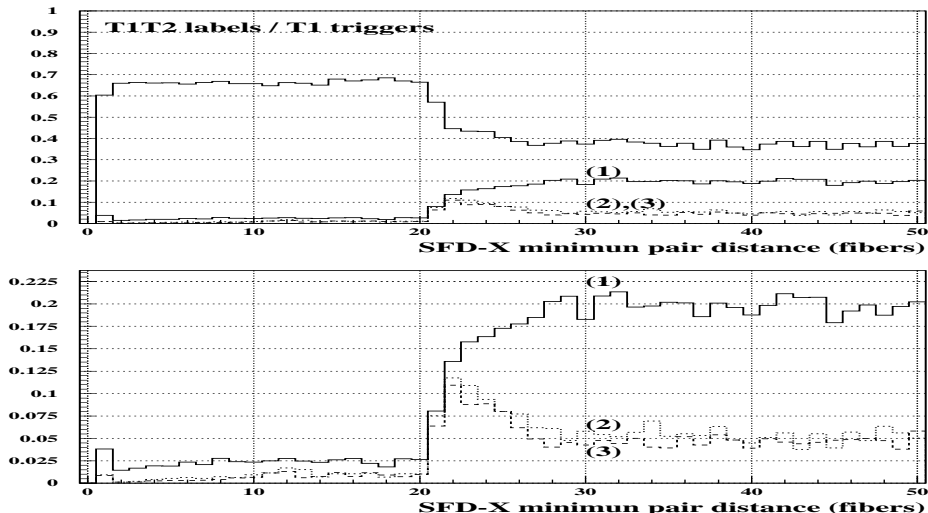


Figure 2: Ratio between T2-labels number and T1-triggers number, function of SFD minimum pair x-distance, ratio T2 type-1/T1 (1), ratio T2 type-2/T1 (2-dashed line) and ratio T2 type-3/T1 (3-dotted line). (The figure at the bottom is the same, with an expanded vertical scale.)

The behaviour changes completely for types-4,5,6,7 as can be seen in figure 3. Here the enhancement at small x-distance is clear but what is more relevant is the contribution of type-4, which means that  $\gtrsim 20\%$  of all T1 triggers have at least one pair with good relative distance but the ionization conditions are not satisfied. This could be due to holes in DE/DX planes or/and SFD-hits out of the acceptance of DE/DX or/and SFD noise-hits. Type-5 shows a peak at small distances while type-6 shows it at larger distances as can be expected from double and single adjacent ionization criteria.

<sup>1</sup>Here the distance is measured in terms hit fibers without use of DC information, this information will be used in the next subsection.

<sup>2</sup>Note that here we consider the detection efficiency for pairs with relative distance  $< 9\text{ mm}$ , no necessarily good T2 events. In any case it should be closer to 100% as it was, at least, during last part of run-II period (see Appendix-I, run 718 data) because T2 works in OR-scheme.

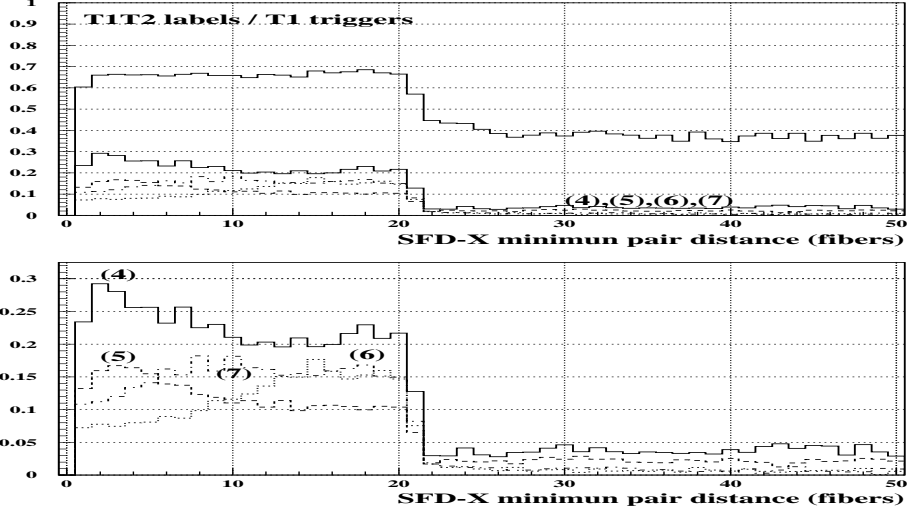


Figure 3: Ratio between T2-labels number and T1 triggers number, function of SFD minimum pair x-distance, ratio T2 type-4/T1 (4), ratio T2 type-5/T1 (5-dashed line), ratio T2 type-6/T1 (6-dotted line) and ratio T2 type-7/T1 (7-dashed-dotted line). (The figure at the bottom is the same, with an expanded vertical scale.)

With the present knowledge, the first reaction would be to remove type-1,2,3 from our data sample or even more work with a T2 AND-scheme<sup>3</sup> instead an OR-scheme. The ratios with respect to T1 trigger appear now like in figure 4. At least for the case of type-4,5,6,7 the situation is more attractive but the acceptance at small  $Q_x$  must be carefully studied. Types-1,2,3 should save atomic pairs with very small x-distance hidden to MODE-III.

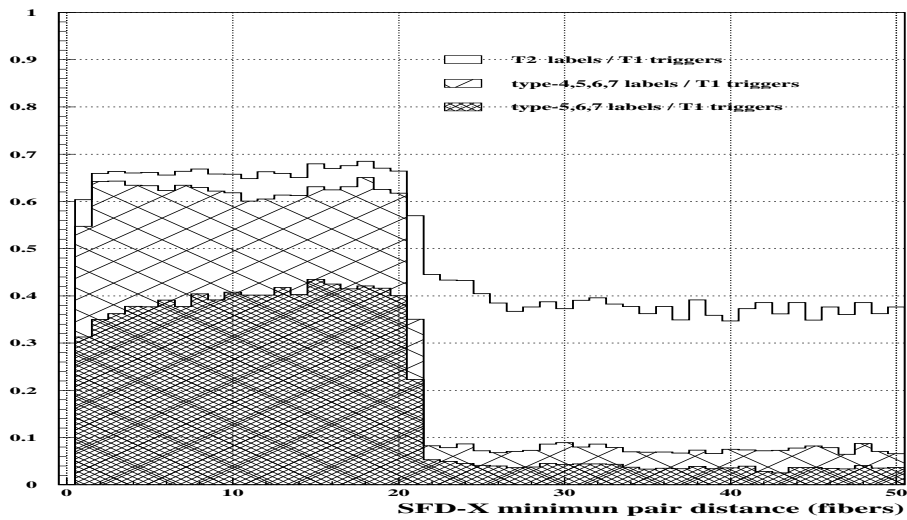


Figure 4: Ratio between T2-labels number and T1-triggers number, function of SFD minimum pair x-distance, ratio T2 type(4+5+6+7)/T1, T2 type(5+6+7)/T1.

<sup>3</sup>An AND scheme means to keep only types 5,6 and 7, [(MODE I OR MODE II) AND MODE III].

Figures 5,6,7,8 show the same analysis in terms of MODE-I, MODE-II, MODE-III to extract the behaviour of T2 trigger if only one of the three modes was activated. Additional information, taking into account time hit constrains is shown in Appendix-II.

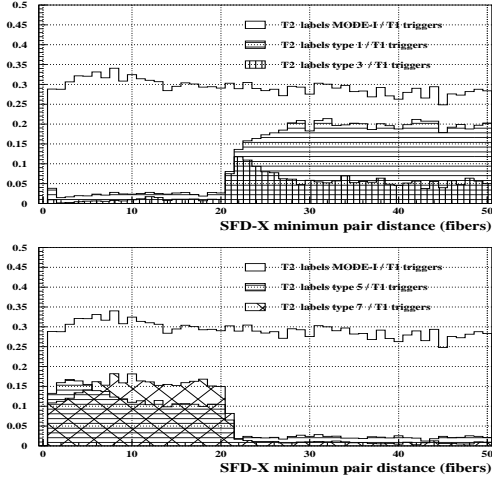


Figure 5: Ratio between T2 MODE-I labels number and T1 triggers number, function of SFD minimum pair x-distance.

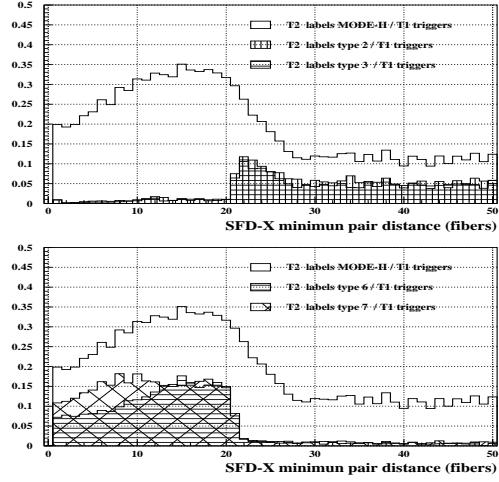


Figure 6: Ratio between T2 MODE-II labels number and T1 triggers number, function of SFD minimum pair x-distance.

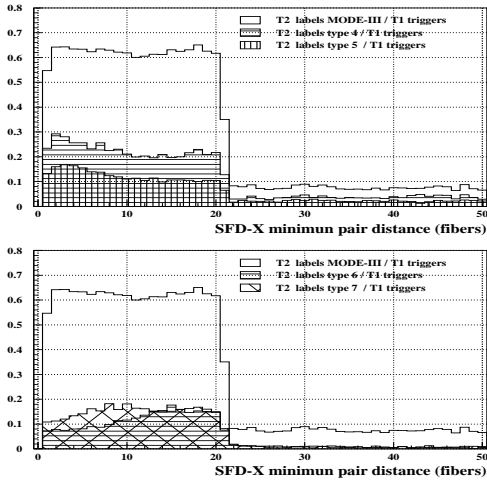


Figure 7: Ratio between T2 MODE-III labels number and T1 triggers number, function of SFD minimum pair x-distance.

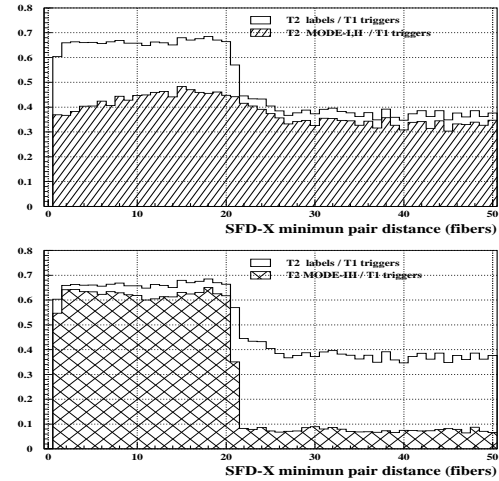


Figure 8: Top: ratio between T2 MODE-(I+II) labels number and T1 triggers number, function of SFD minimum pair x-distance. Bottom: ratio T2 MODE-III/T1.

## 2.2 SFD-X distances and $Q_x$ distributions

It is easy to recognize that the x-distance distributions shown in the previous section are directly correlated with  $Q_x$  distributions and the implications of this in the  $A_{2\pi}$  detection. Figure 9 represents this correlation for the different T2 types.

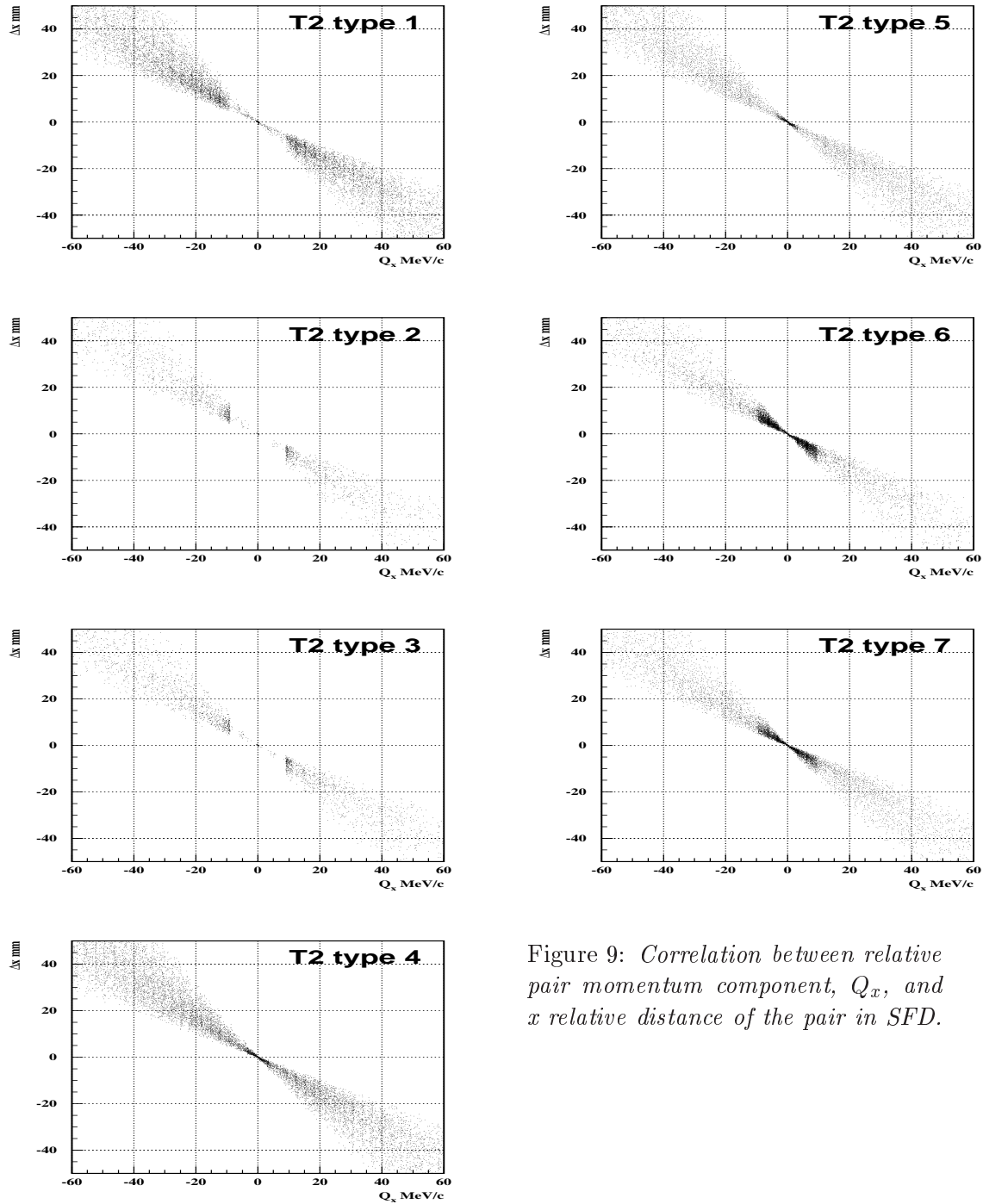


Figure 9: *Correlation between relative pair momentum component,  $Q_x$ , and x relative distance of the pair in SFD.*

For the good-pair events the  $Q_x$  relative momentum component is plotted versus the x relative distance of the pair in SFD. Only types 5,6 and 7 exhibit a clear enhancement in the region of small  $Q_x$ , which is not the case of type-4. Meanwhile types 1,2,3 are highly inefficient in the same region. The importance of this observation must be considered in accordance with the  $Q_x$  distribution for the  $A_{2\pi}$  pairs presented in figure 10 and obtained with Monte Carlo simulation in which multiple scattering of particles in target and MSGC detectors was taken into account.

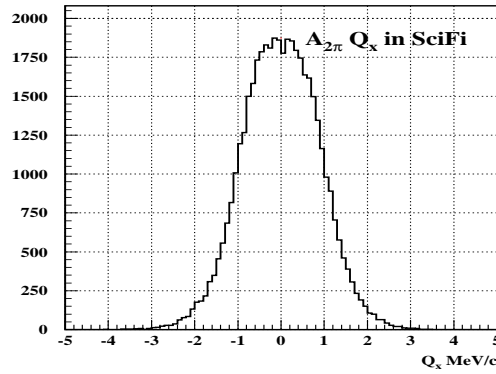


Figure 10:  $Q_x$  distribution of  $A_{2\pi}$  pion pairs.

Finally, figure 11 establishes the T2-efficiency for detection of pairs with low  $Q_x$  relative momentum as well as background rejection. The contribution of types 1,2,3,4 can also be extracted from the plots. A detailed study is summarized in figures 12,13,14,15. The almost uniform acceptance in  $Q_x$  of T2 contrasts with the inefficiency of T2 MODE-I,II and T2 MODE-III in the central region. The contribution at small  $Q_x$  of T2-type 1 is clear as well the contamination at large  $Q_x$  also present in T2-type 4.

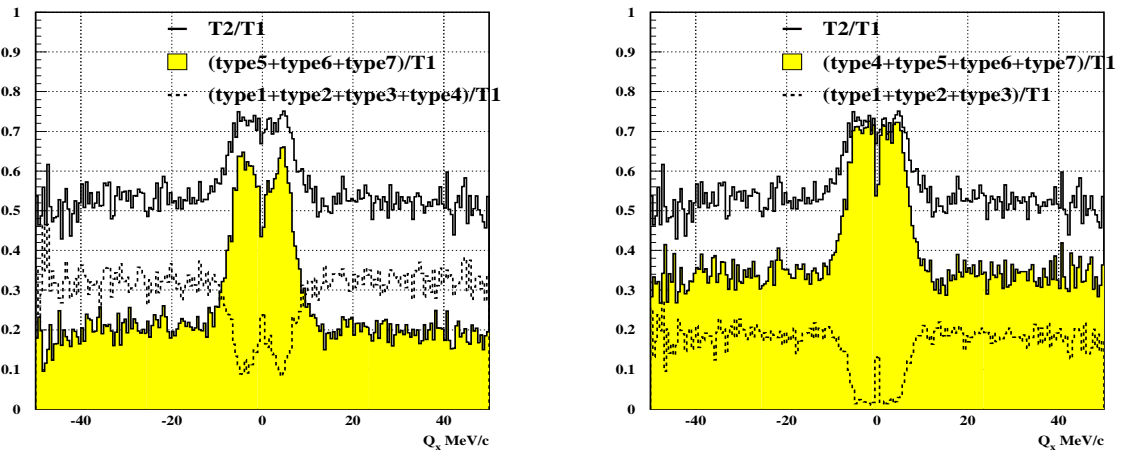


Figure 11: Ratios between T2 marks and T1 triggers for the  $Q_x$  distribution.

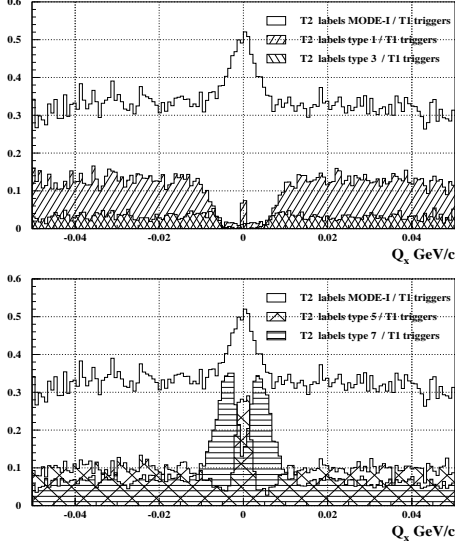


Figure 12: Ratio between  $T2$  MODE-I marks and  $T1$  triggers for the  $Q_x$  distribution of good-pair events.

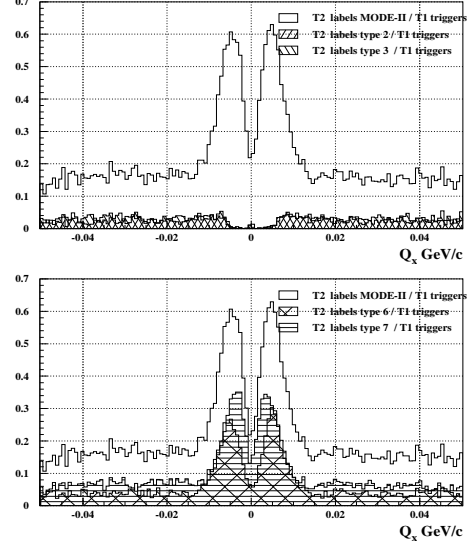


Figure 13: Ratio between  $T2$  MODE-II marks and  $T1$  triggers for the  $Q_x$  distribution of good-pair events.

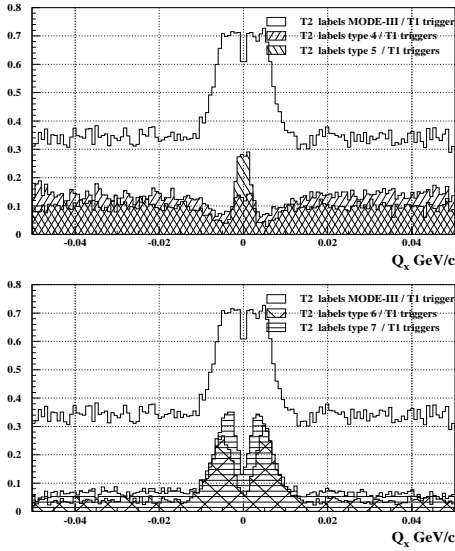


Figure 14: Ratio between  $T2$  MODE-III marks and  $T1$  triggers for the  $Q_x$  distribution of good-pair events.

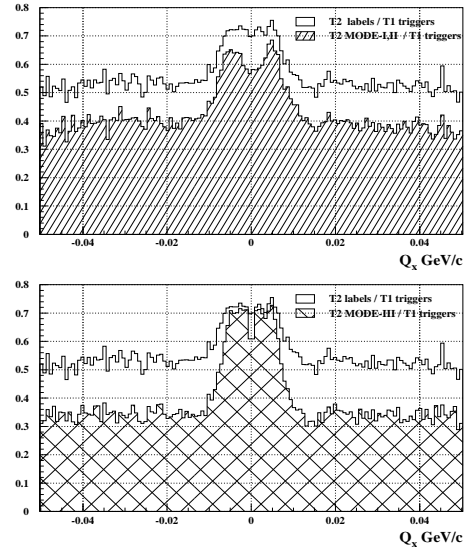


Figure 15: Top: ratio between  $T2$  MODE-I,II marks and  $T1$  triggers for the  $Q_x$  distribution of good-pair events. Bottom: ratio between  $T2$  MODE-III and  $T1$  triggers.



## 2.3 Expected behaviour of T2 from simulation

### 2.3.1 Understanding the experimental data

In order to better understand the results that we get from the experimental data, the T2 trigger behaviour has been simulated using the information from DE/DX and SFD detectors. The DE/DX amplitude spectra and time information was used to simulate the double (MODE-I) and single adjacent (MODE-II) ionization criteria. Double and single threshold cuts have been fixed to a common value for all the slabs and they have been adjusted to the best fit between experimental and simulated results.

SFD-plane information recorded for tracking was used in “OR” of two fibers trying to reproduce the answer of TLC and hence the mark  $< 9\text{ mm}$  (MODE-III) as well as the SFDveto(9-13mm). The results of the already described simulation are presented in figure 16 and figure 17 for the seven different possible combinations of T2 trigger modes.

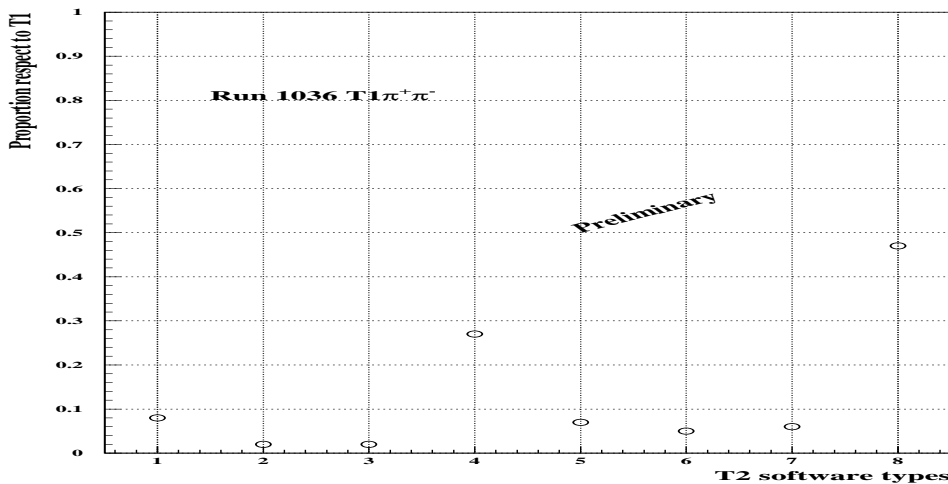


Figure 16: Rates of different T2-types obtained by software simulation normalised to the initial T1 triggers. The bin number 8 means the proportion of T1 triggers without T2-marks.

Figure 16 shows that the simulated ratios of the different T2 types coincide with the experimental data except for type 4. As can be seen in figure 17 types 1,2 and 3 show a similar behaviour below and above minimum relative distance equals to 20 fibers. Above 20 fibers, the simulation reproduces quite well the experimental data<sup>4</sup> and the contribution of this modes in this region is pure background. Below 20 fibers we found events with hits in SFD-X at correct distance that are not detected by TLC. The ored signals at the input of TLC can only explain part of the peak at distance equal to 1 fiber (see figure 18), the rest could be inefficiencies of TLC; in any case they are less than 4%. The enhancement above 20 fibers in modes 2 and 3, is due to the absence of SFDveto(9-13mm).

<sup>4</sup>Remember that an individual slab threshold adjustment was not performed, two signal branches (NIM and CAMAC) for DE/DX are not ideal to make this fine tuning.

The experimental type-4 data are clearly not compatible with those expected by simulation. The simulation calculates a 13% excess for triggers of this type. What is unclear up to now is the nature of these triggers.

Types 5, 6 and 7 are in reasonable agreement with the simulation results. The differences should come from a non perfect tuning of thresholds in DE/DX as well as from the unknown reason that originates inefficiencies in TLC in types 1,2,3.

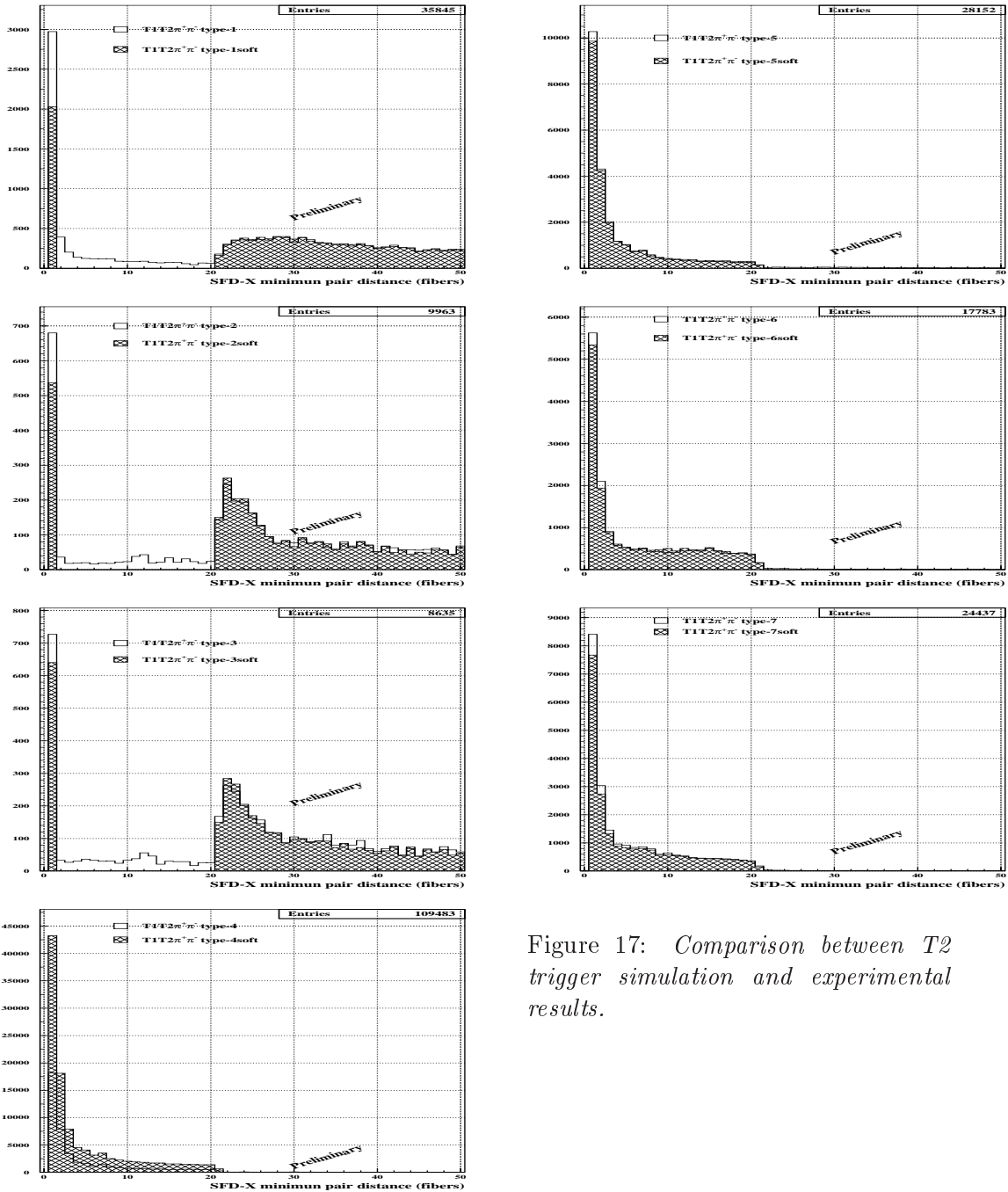


Figure 17: Comparison between  $T_2$  trigger simulation and experimental results.

Figure 18, shows the effect after suppression of the 'OR' in the TLC inputs.

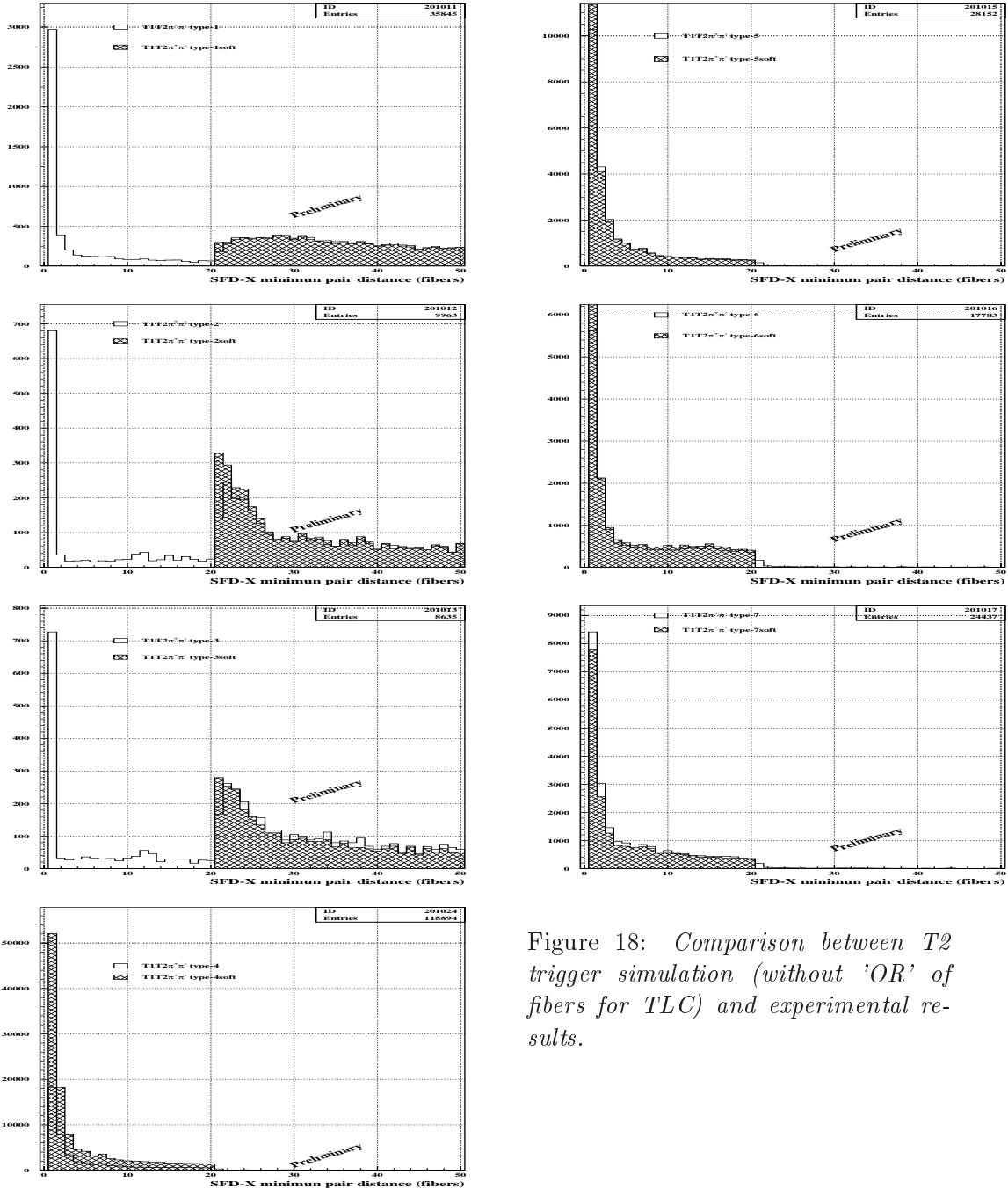


Figure 18: Comparison between T2 trigger simulation (without 'OR' of fibers for TLC) and experimental results.

### 2.3.2 Effect of increase the double ionization threshold

During the last DIRAC run it was proposed to increase the double ionization threshold in DE/DX detector and improve in this way the quality of our data. The result of this action can be predicted with the simulation already tuned for the best fit with the experimental

data. The value of the double ionization cut used in simulation can be increased from 250 to 300 channels in ADC spectra and the results are summarized in the figure 19.

The increase of T2 reduction factor produces a growth of type-4 and a suppression of types 1,3,5,7. The new incoming triggers of type-4 are not able to satisfy the ionization criteria and so they are clearly not good. This could be an indication that most of the original type-4 are in fact also not good. Type 1 and 3 appear now suppressed but the tails at large minimum x-distance are still there (see figure 20). The last of the most important effects of this proposal is the new proportion between type 5 and 6, and also between type

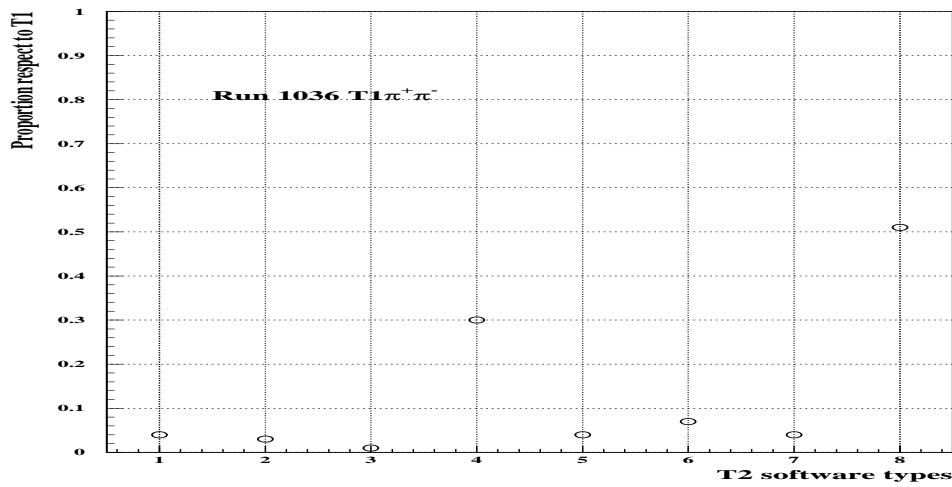


Figure 19: Rates of different T2-types obtained by software simulation with respect to the initial T1 triggers, after increasing the double ionization cut. The bin number 8 means the proportion of T1 triggers without T2-mark.

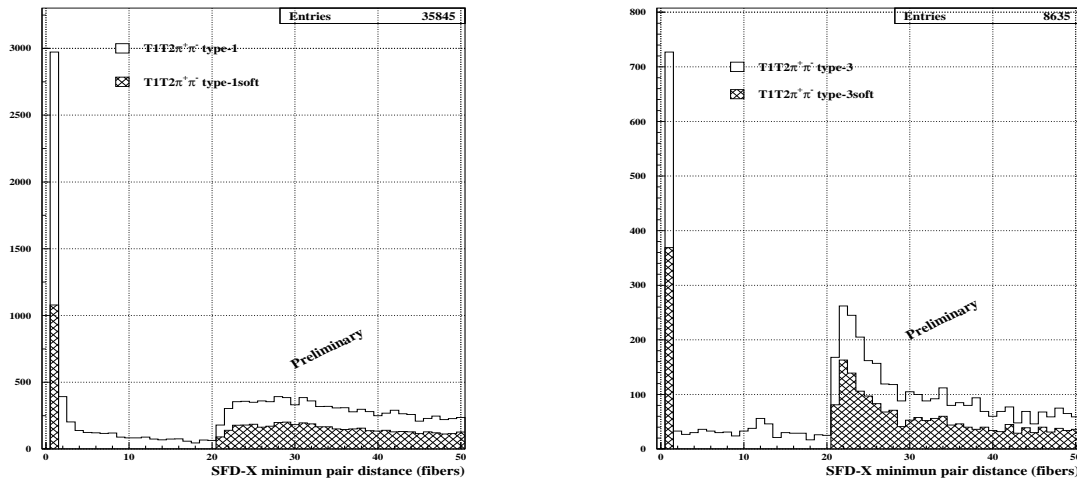


Figure 20: Results of the simulation after increasing the double ionization cut.

7 and 6. Now it is established that the predominant situation of the type 6 and its very low  $Q_x$  inefficiency, possible bias in the  $Q_x$ , acceptance has to be studied.

## 2.4 SFD-X distances equal to 0 and 1 fiber

In sections 2.1 and 2.3 distances between hits equal to zero have been removed in all the plots because it is obvious that the TLC is not able to detect them. Distances zero in terms of hit fibers appear in events with only 1 hit in SFD x-plane ( $\sim 0.2\%$ ) or in situations in which there are more than 1 hit, but 2 of them fired the same fiber ( $\sim 0.005\%$ ), SFD electronics is able to resolve them in time, and so zero is the minimum distance in the algorithm that we are using. Apart from the very small number of this latter case, the time distance for the hits that fired the same fiber is  $> 30 ns$ .

As far as 1 fiber distances are concerned the experimental data show a large proportion of this type of minimum distances (see fig 17), near to the granularity of SFD and TLC trigger system. Figure 21 shows the x-coordinate distribution for 1 hit of the pair when the relative distance is one fiber. Clearly a periodical structure of 32 fibers is present and another periodical structure of 16 fibers could be also present. It is clear that the peaks cannot explain such number of events with minimum distance equal 1 but they are unpleasant from the point of view of tracking as well as trigger, if they are also present in the trigger electronics. Figure 21 shows pure T1 triggers without influence of T2 trigger, so the origin of this structure must be at the level of SFD detector, PMTs or PSC. Moreover, although their statistic is small, modes 1,2 and 3 seem not to show such a structure.

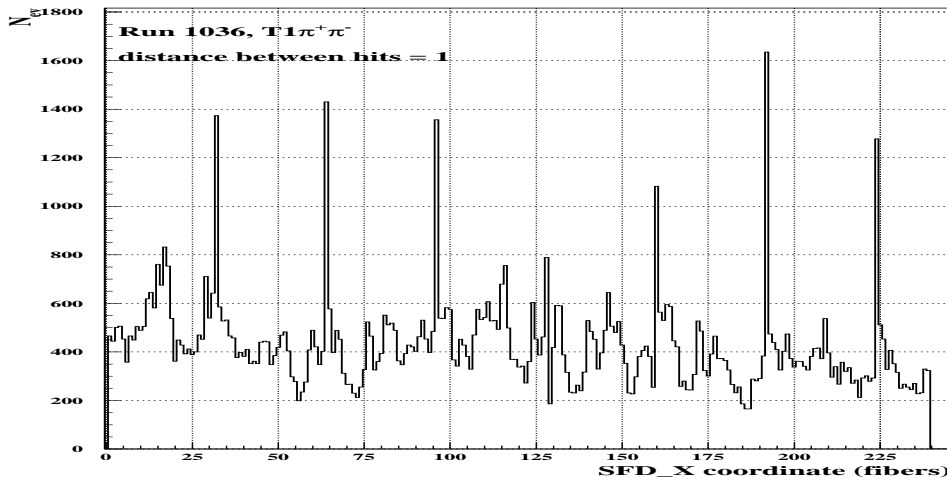


Figure 21:  $x$ -distribution for one of the hits of the pairs with relative distance equal to one.

## 3 The effect of multiplicity on T2 modes

It is obvious that multiplicity is one of the main difficulties that a trigger system must overcome. In particular for the T2 trigger of our experiment, which aims at selecting low

$Q_x$  particle pairs, looking for pair of hits with small x-relative distance. It is easy to see that if the multiplicity at the x-plane of SFD equals  $n$  the number of possible particle pairs that we can compose with these  $n$  particles is equal to  $n(n - 1)/2$ . Figure 22 shows how the number of possible pairs with relative x-distance  $< 9\text{ mm}$  increase with multiplicity on SFD-x detector.

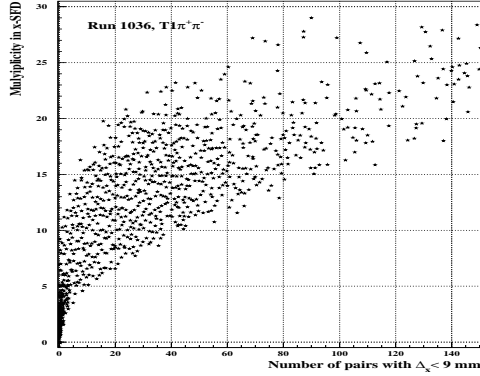


Figure 22: *Multiplicity on SFD x-plane vs number of possible pairs with x-distance  $< 9\text{ mm}$ .*

The behaviour of each T2 type with the multiplicity is also an important characteristic to decide which is the best one. Figure 23(a) shows this characteristic for all T2 types in terms of SFD multiplicity. Types 1,2 or 3 have importance at low multiplicity or even zero and their contribution to increase the number of pairs  $x < 9\text{ mm}$  is very small (see fig 23(b)). Zero multiplicity is also present in types which include SFD decision.

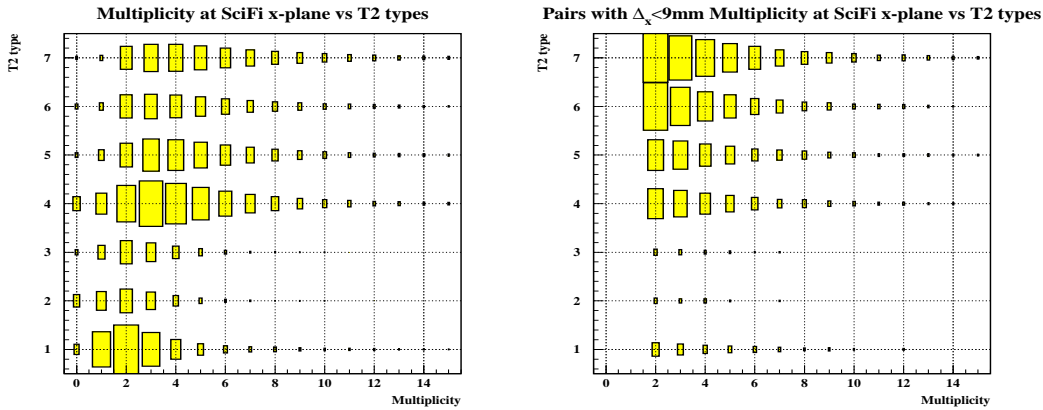


Figure 23: *Multiplicity on SFD x-plane for the different T2 modes: (a) all T1 triggers, (b) T1 triggers with one good-pair event.*

In terms of DE/DX multiplicity the above types look like it is shown in figure 24. Here the difficulties to establish where are the single and double ionization thresholds for each slab makes difficult to extract conclusions, but it seems that T2-type 1 corresponds to not so large double multiplicity in DE/DX detector and small multiplicity in SFD. Type 1 could save pairs that fired one fiber and the tails at large distances probably have

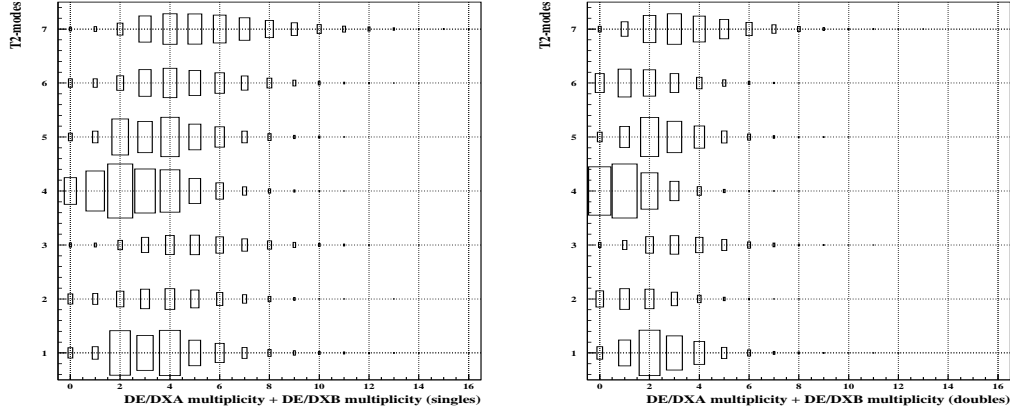


Figure 24: *Multiplicity on DE/DX planes for the different T2 modes.*

their origin in the improper tuning of double ionization threshold. For T2 type-4 DE/DX signals are present but seems that they are not able to fulfill the ionization criteria in the single adjacent version or in the double ionization one.

To go deeper in the understanding of these types behaviour with multiplicity we have calculated the x-coordinate of the extrapolated negative arm track, at the x-plane of SFD, minus the corresponding extrapolation of the positive arm track for several values of multiplicity.

In figure 25 we can see the x-distance for the reconstructed pairs in case of type 1. Multiplicity cases, from 2 to 6 have been considered. The main comment about this specific type is due to the large amount of pairs with relative distance greater than 9 mm. This fact has not an easy explanation but could be in the DE/DX double ionization criterion itself. Sometimes an unique particle could lose enough energy in one slab of DE/DX and verify the double ionization criterion (tail of the Landau distribution). In this case the second particle of the pair could be at less than 9 mm (type 5) or at long distances (type 1).

Analogues to figure 25, figures 26 and 27 are shown for types 2 and 3. As these are also pure DE/DX type low multiplicity plots have more entries. For these two types it is clear that as multiplicity increases the relative proportion of events outside of the 18 mm width central gap is higher.

For the other types, the effect of multiplicity on the degradation of the quality of the particle pairs is evident. The case with multiplicity equal to 2, and maybe 3 in some of the types, is the only in which the central region is clearly enhanced. A special mention is in order for type 4 where the behaviour is acceptable only for multiplicity 2.

One final remarkable characteristic is that types 6 and 7, in which both SFD and DEDX participate in trigger, show an important enhancement of the central region even if the multiplicity is high.

## T2 type 1

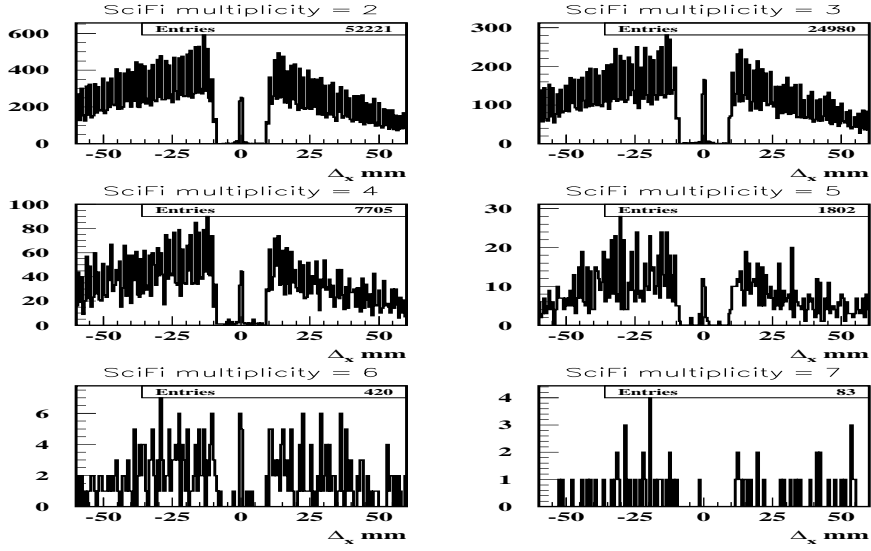


Figure 26: *Difference in  $x$  for the particles of a reconstructed pair at plane  $x$  of SFD. Pairs with T2 type 2.*

## T2 type 2

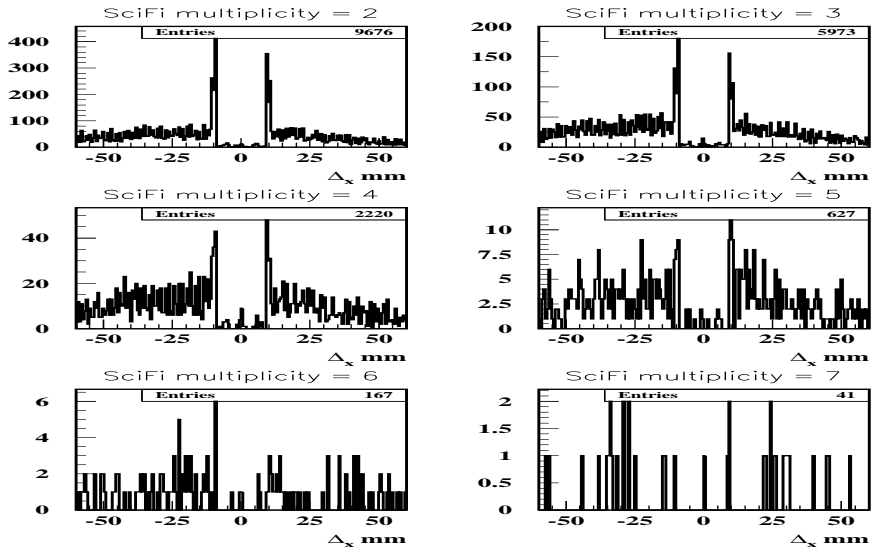


Figure 25: *Difference in  $x$  for the particles of are constructed pair at plane  $x$  of SFD. Pairs with T2 type 1.*



### T2 type 3

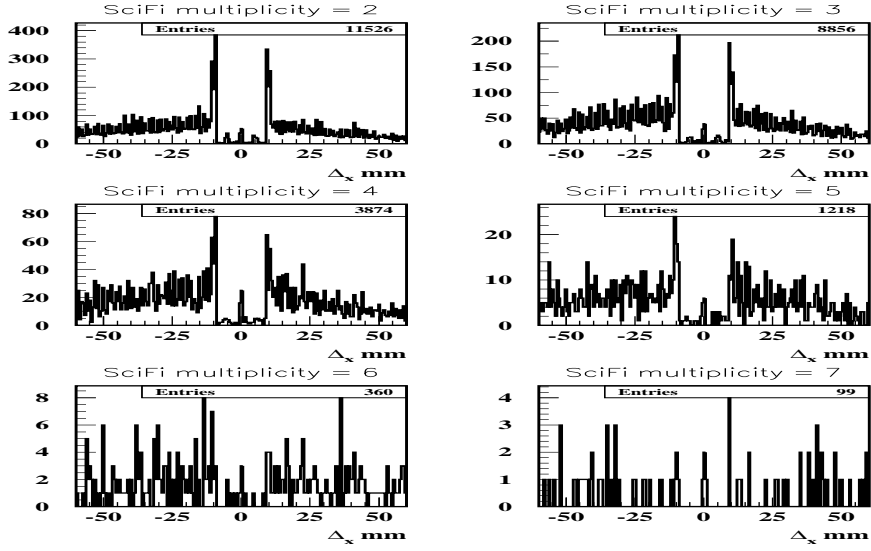


Figure 27: *Difference in  $x$  for the particles of a reconstructed pair at plane  $x$  of SFD. Pairs with T2 type 3.*

### T2 type 4

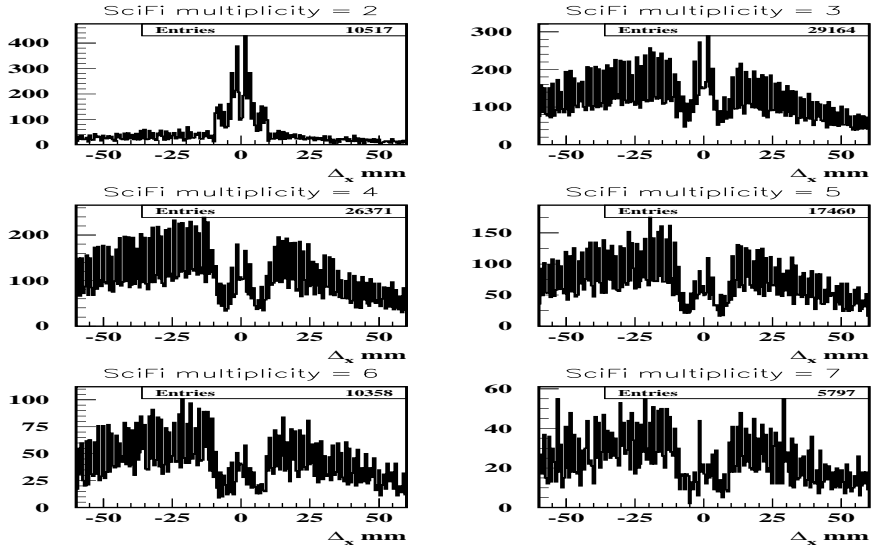


Figure 28: *Difference in  $x$  for the particles of a reconstructed pair at plane  $x$  of SFD. Pairs with T2 type 4.*

## T2 type 5

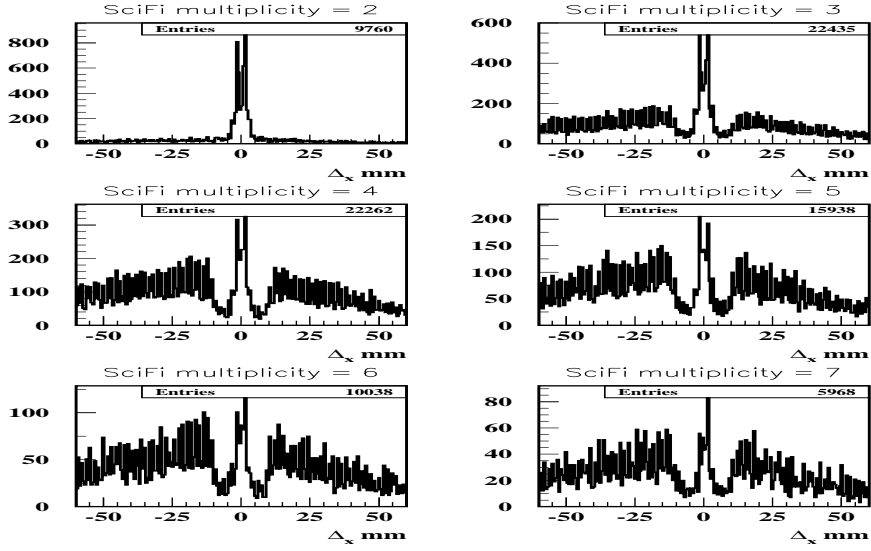


Figure 29: *Difference in  $x$  for the particles of a reconstructed pair at plane  $x$  of SFD. Pairs with T2 type 5.*

## T2 type 6

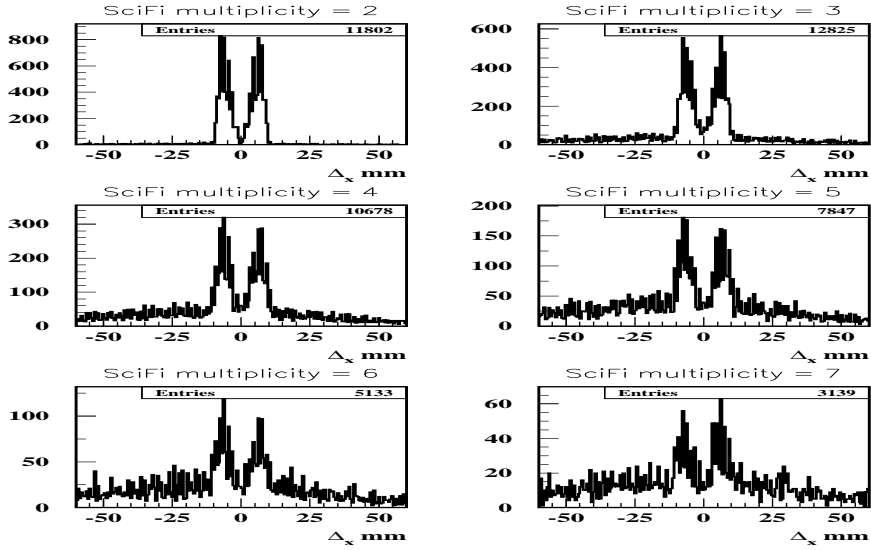


Figure 30: *Difference in  $x$  for the particles of a reconstructed pair at plane  $x$  of SFD. Pairs with T2 type 6.*

## T2 type 7

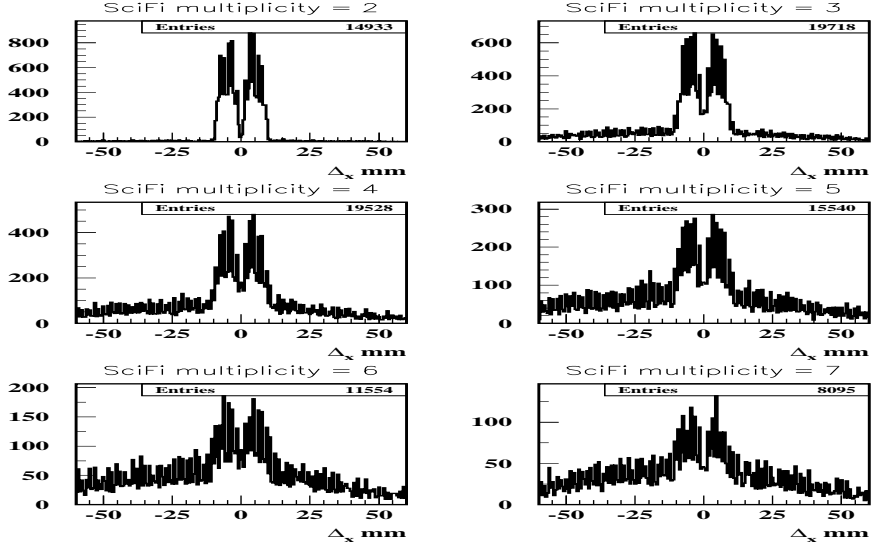


Figure 31: *Difference in x for the particles of a reconstructed pair at plane x of SFD. Pairs with T2 type 7.*

## 4 T2-type 4 and the DE/DX amplitude spectra

The DE/DX amplitude spectra can be studied in a clearer and cleaner way selecting events with multiplicity one in each DE/DX plane and in such a way that the fired slab numbers in both planes coincide.

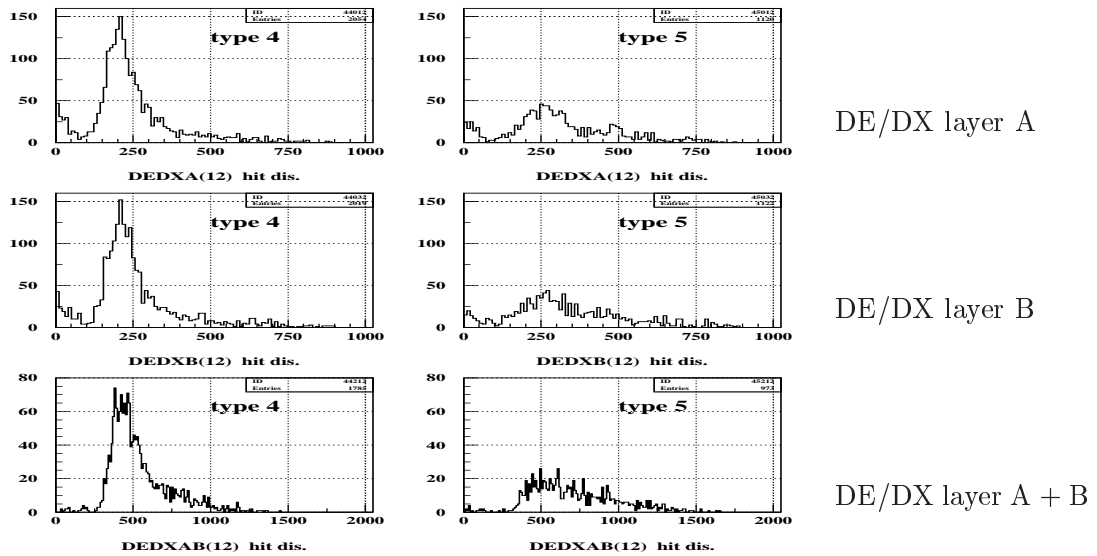


Figure 32: *DE/DX amplitude spectra for types 4 and 5.*

This is shown for the slab 12, using the data recorded in runs 1036, 1037 and 1276, in figure 32. Type 4 has a mean value below 250 channels or below 500 channels if we add the amplitudes in layer A and B. Clearly most of the times type-4 selects events with low ionization. One point that is not clear is why events with amplitude spectra over 500 channels were marked as type 4 and not as type 5.

## 5 Appendix-I:

The most representative plots already shown for run 1036 are reproduced now for run 718 in which the global efficiency of T2 for selection of pairs with distance  $< 9\text{ mm}$  is near to 90 % (instead of 70 % for the run 1036).

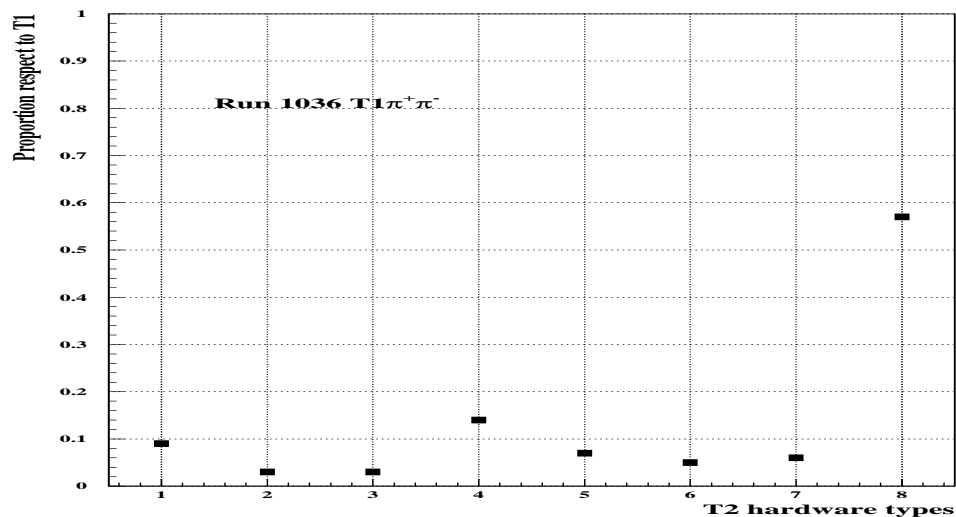


Figure 33: Rates of different T2-types with respect to the initial T1 triggers. The bin number 8 means the proportion of T1 triggers without T2-marks.

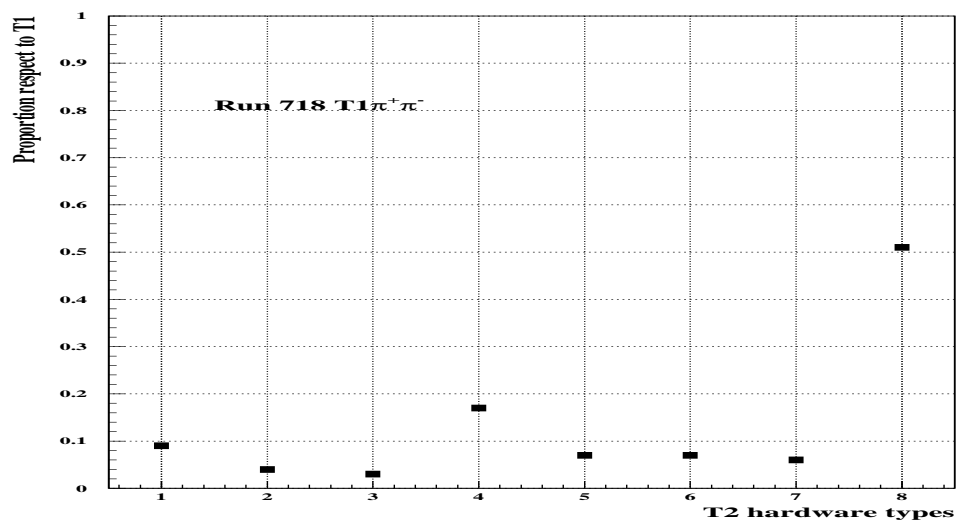


Figure 34: Rates of different T2-types with respect to the initial T1 triggers. The bin number 8 means the proportion of T1 triggers without T2-marks.

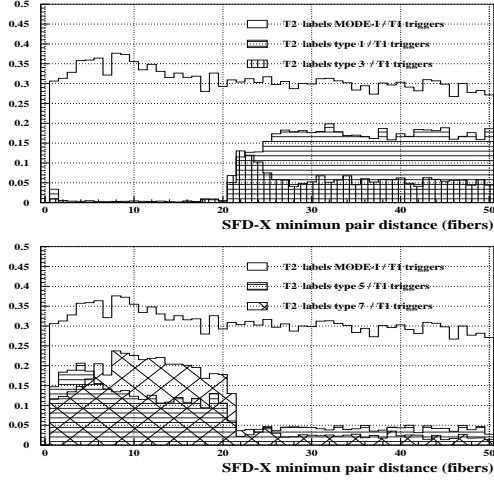


Figure 35: Ratio between  $T2$  MODE-I labels number and  $T1$  triggers numbers, function of SFD minimum pair  $x$ -distance (run 718).

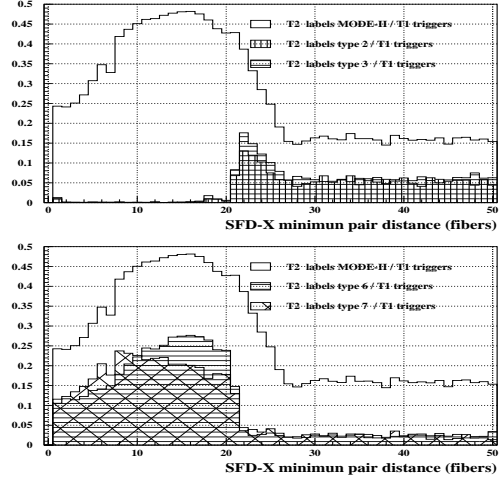


Figure 36: Ratio between  $T2$  MODE-II labels number and  $T1$  triggers numbers, function of SFD minimum pair  $x$ -distance (run 718).

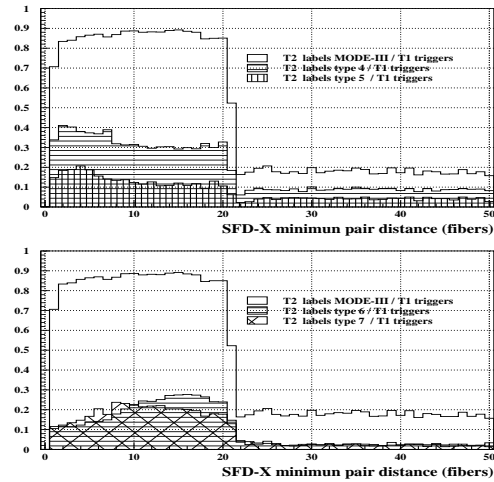


Figure 37: Ratio between  $T2$  MODE-III labels number and  $T1$  triggers numbers, function of SFD minimum pair  $x$ -distance (run 718).

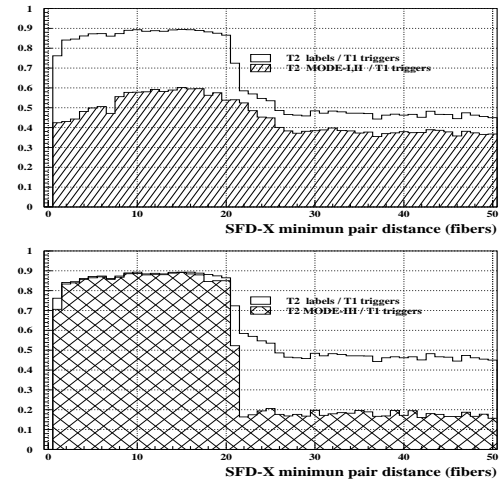


Figure 38: Top: ratio between  $T2$  MODE-(I+II) labels number and  $T1$  triggers number, function of SFD minimum pair  $x$ -distance. Top: ratio  $T2$  MODE-III/ $T1$  (run 718).

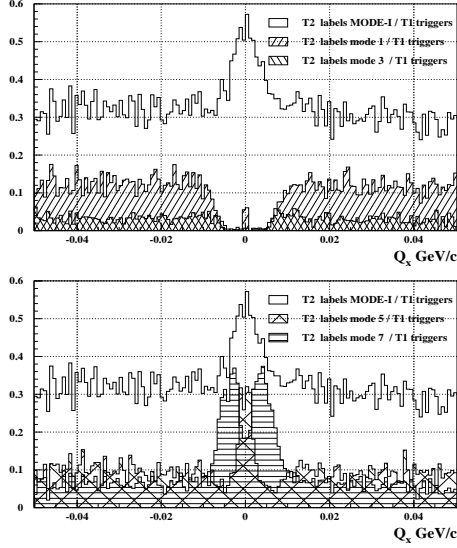


Figure 39: Ratio between  $T2$  MODE-I marks and  $T1$  triggers for the  $Q_x$  distribution of good-pair events (run 718).

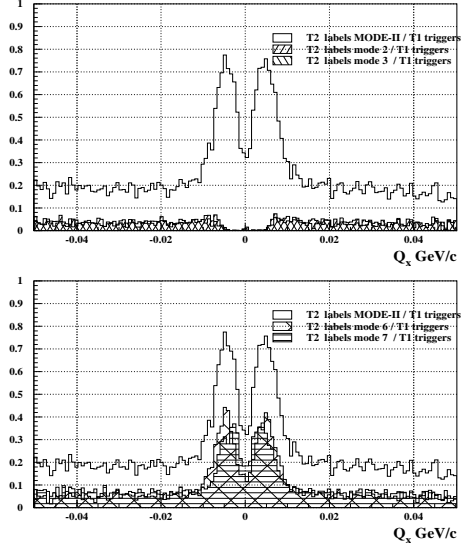


Figure 40: Ratio between  $T2$  MODE-II marks and  $T1$  triggers for the  $Q_x$  distribution of good-pair events (run 718).

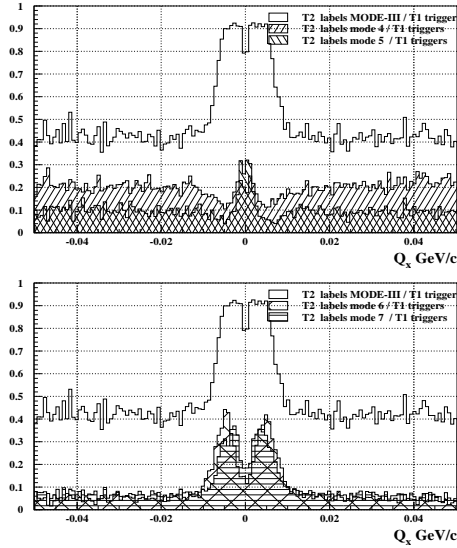


Figure 41: Ratio between  $T2$  MODE-III marks and  $T1$  triggers for the  $Q_x$  distribution of good-pair events (run 718).

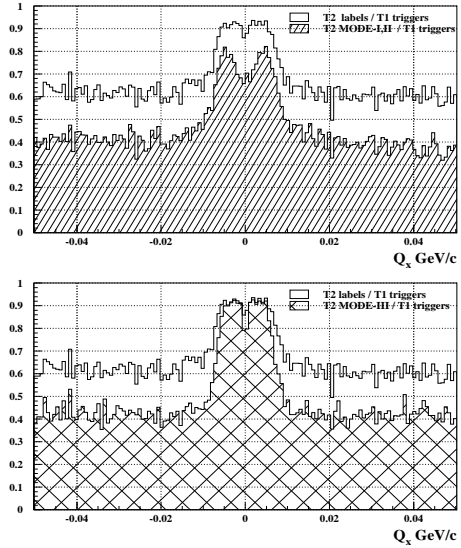


Figure 42: Top: ratio between  $T2$  MODE-I,II marks and  $T1$  triggers for the  $Q_x$  distribution of good-pair events. Bottom: ratio between  $T2$  MODE-III and  $T1$  triggers (run 718).

## 6 Appendix-II:

The same analysis shown in figures 5,6,7,8 is reproduced for the same data (run 1036) but imposing now time constrains for the accepted hits in our data sample. Now we will only take into account two hits if their time difference is less than 20 ns, 15 ns, 10 ns, 5 ns, or 2 ns.

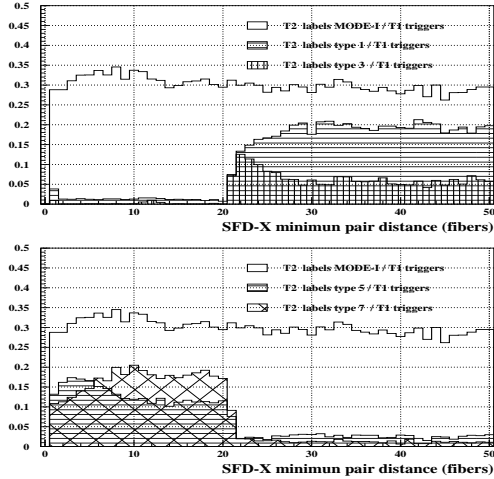


Figure 43: Ratio between  $T2$  MODE-I labels number and  $T1$  triggers number, function of SFD minimum pair  $x$ -distance (time constrain 20 ns).

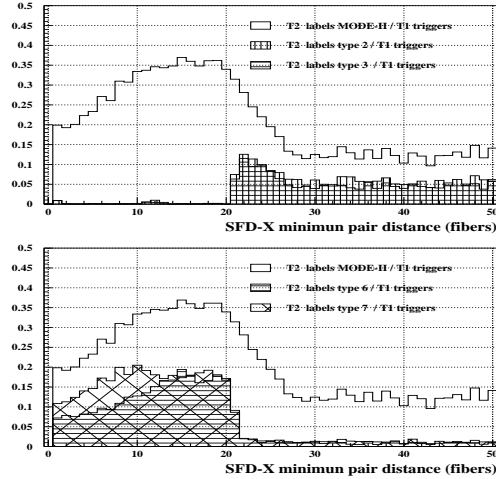


Figure 44: Ratio between  $T2$  MODE-II labels number and  $T1$  triggers number, function of SFD minimum pair  $x$ -distance (time constrain 20 ns).

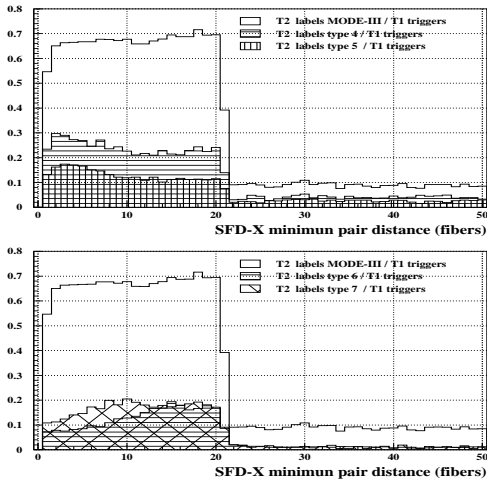


Figure 45: Ratio between  $T2$  MODE-III labels number and  $T1$  triggers number, function of SFD minimum pair  $x$ -distance (time constrain 20 ns).

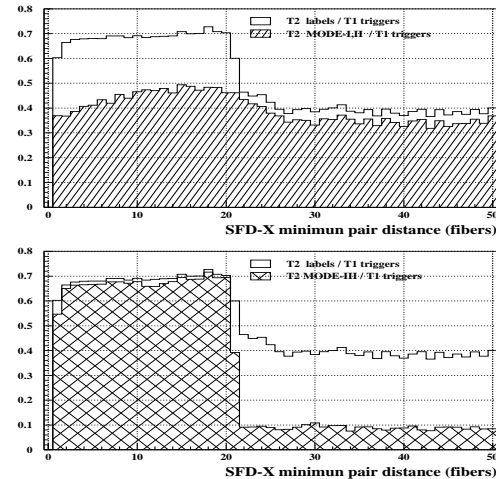


Figure 46: Top: ratio between  $T2$  MODE-(I+II) labels number and  $T1$  triggers number, function of SFD minimum pair  $x$ -distance. Bottom: ratio  $T2$  MODE-III/ $T1$  (time constrain 20 ns).



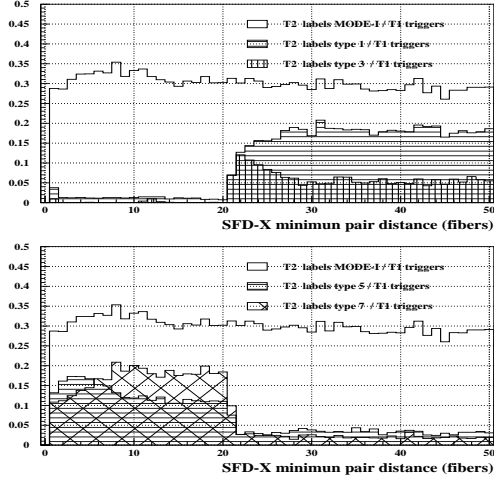


Figure 47: Ratio between  $T2$  MODE-I labels number and  $T1$  triggers number, function of SFD minimum pair  $x$ -distance (time constrain 15 ns).

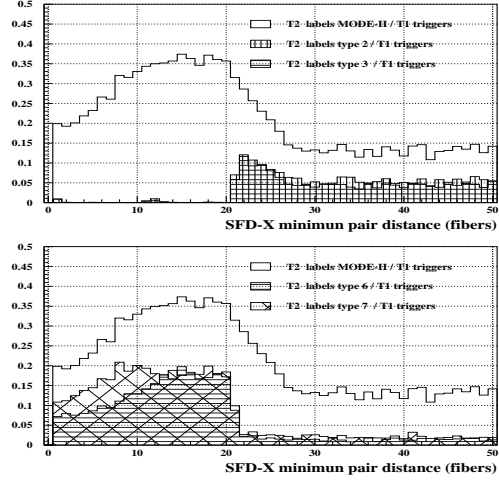


Figure 48: Ratio between  $T2$  MODE-II labels number and  $T1$  triggers number, function of SFD minimum pair  $x$ -distance (time constrain 15 ns).

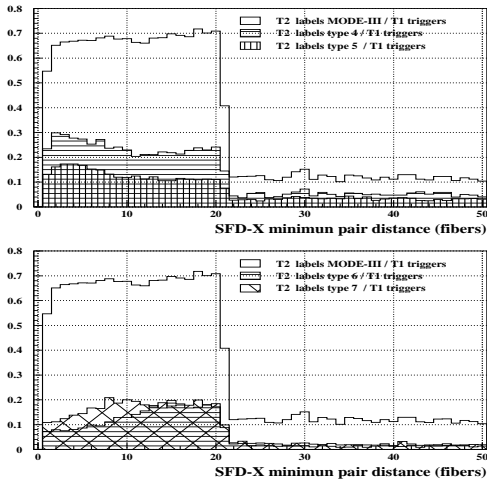


Figure 49: Ratio between  $T2$  MODE-III labels number and  $T1$  triggers number, function of SFD minimum pair  $x$ -distance (time constrain 15 ns).

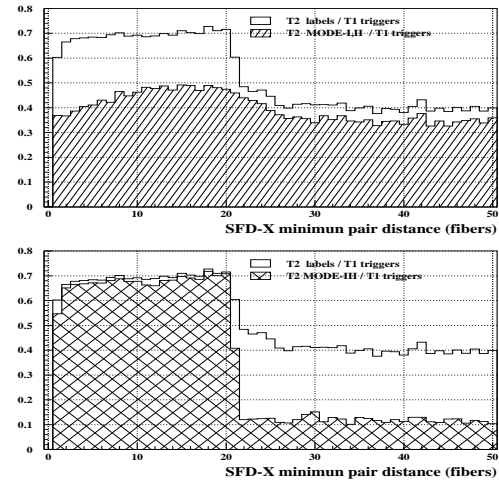


Figure 50: Top: ratio between  $T2$  MODE-(I+II) labels number and  $T1$  triggers number, function of SFD minimum pair  $x$ -distance. Bottom: ratio  $T2$  MODE-III/ $T1$ . the pairs (time constrain 15 ns).

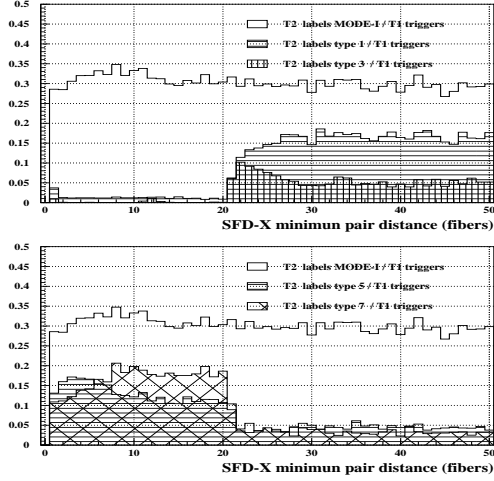


Figure 51: Ratio between  $T2$  MODE-I labels number and  $T1$  triggers number, function of SFD minimum pair  $x$ -distance.

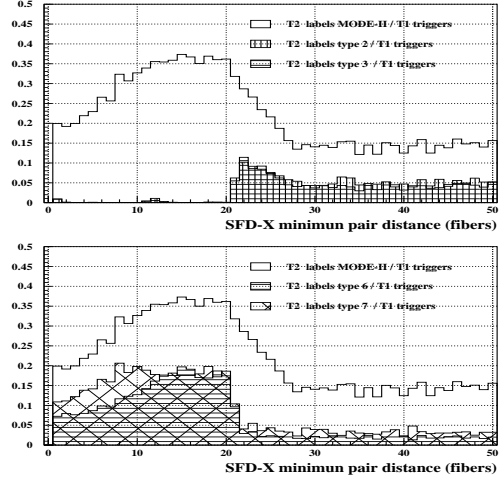


Figure 52: Ratio between  $T2$  MODE-II labels number and  $T1$  triggers number, function of SFD minimum pair  $x$ -distance (time constrain 10 ns).

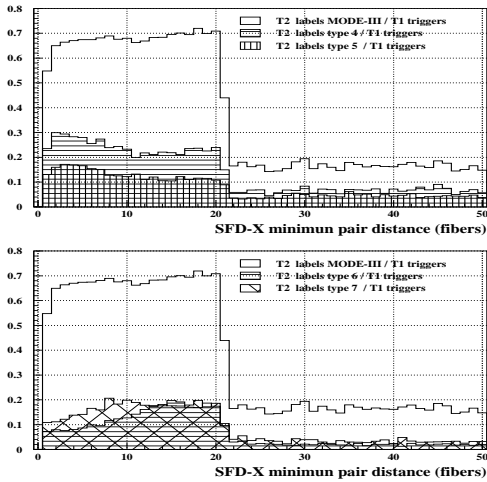


Figure 53: Ratio between  $T2$  MODE-III labels number and  $T1$  triggers number, function of SFD minimum pair  $x$ -distance (time constrain 10 ns).

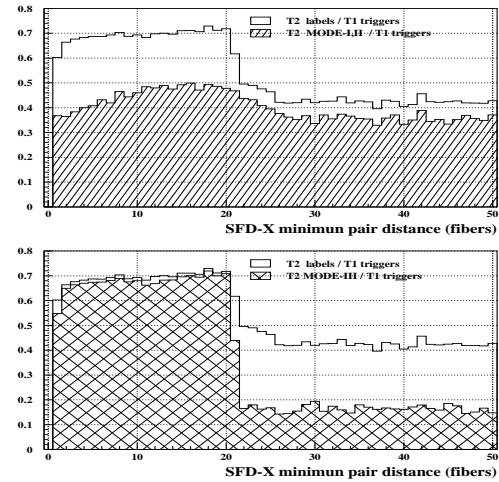


Figure 54: Top: ratio between  $T2$  MODE-(I+II) labels number and  $T1$  triggers, function of SFD minimum pair  $x$ -distance. Bottom: ratio  $T2$  MODE-III/ $T1$  (time constrain 10 ns).

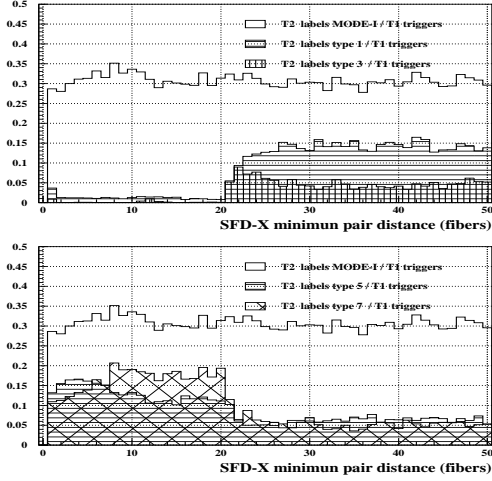


Figure 55: Ratio between  $T2$  MODE-I labels number and  $T1$  triggers number, function of SFD minimum pair  $x$ -distance (time constrain 5 ns).

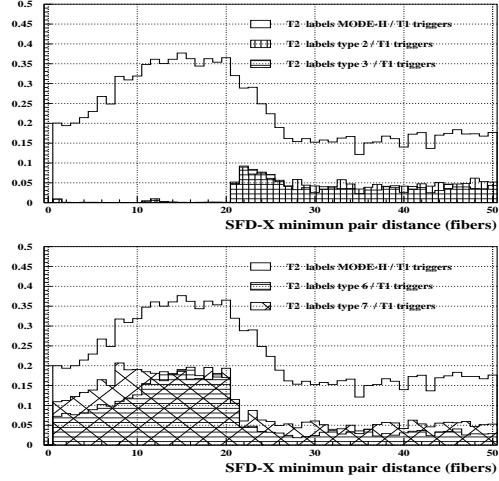


Figure 56: Ratio between  $T2$  MODE-II labels number and  $T1$  triggers number, function of SFD minimum pair  $x$ -distance (time constrain 5 ns).

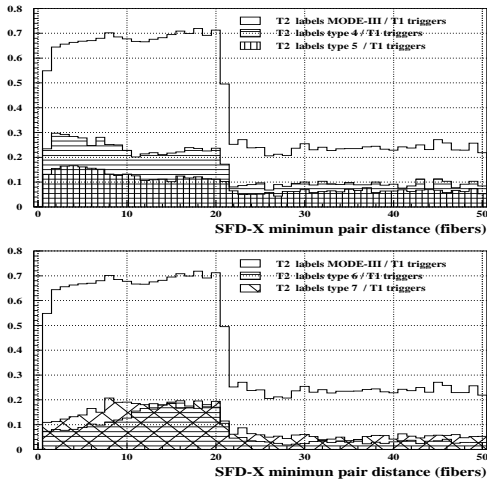


Figure 57: Ratio between  $T2$  MODE-III labels number and  $T1$  triggers number, function of SFD minimum pair  $x$ -distance (time constrain 5 ns).

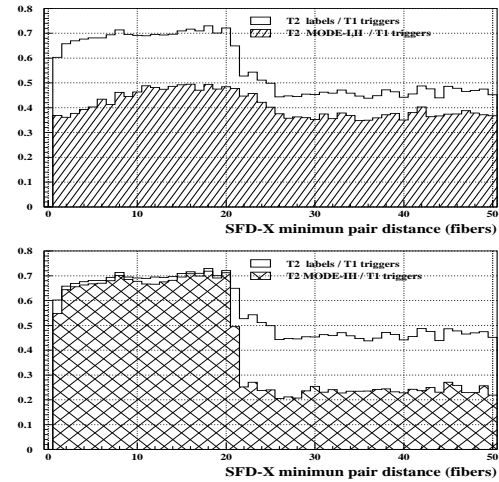


Figure 58: Top: ratio between  $T2$  MODE-(I+II) labels number and  $T1$  triggers number, function of SFD minimum pair  $x$ -distance. Bottom: ratio between  $T2$  MODE-III/ $T1$  (time constrain 5 ns).

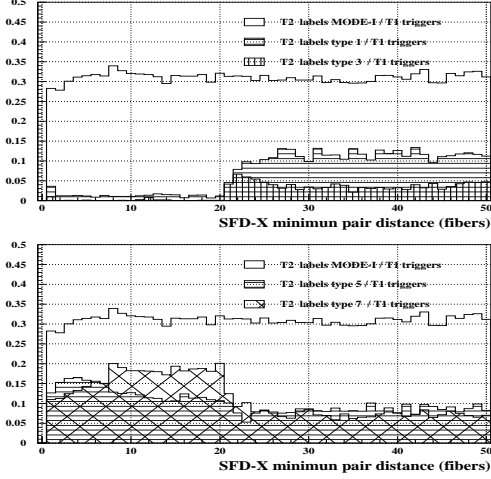


Figure 59: Ratio between  $T2$  MODE-I labels number and  $T1$  triggers number, function of SFD minimum pair  $x$ -distance (time constrain 2 ns).

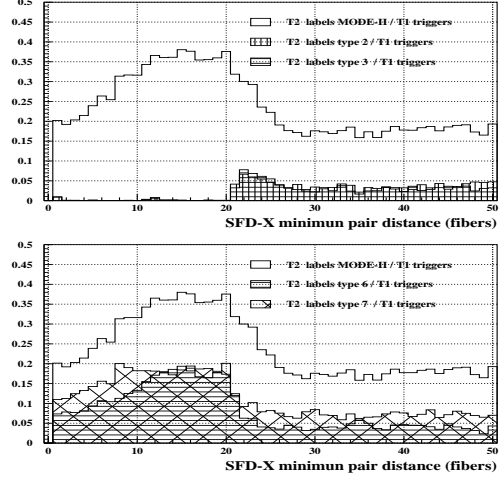


Figure 60: Ratio between  $T2$  MODE-II labels number and  $T1$  triggers number, function of SFD minimum pair  $x$ -distance (time constrain 2 ns).

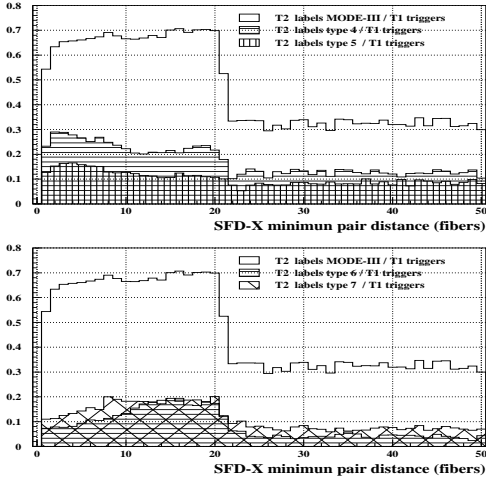


Figure 61: Ratio between  $T2$  MODE-III labels number and  $T1$  triggers number, function of SFD minimum pair  $x$ -distance (time constrain 2 ns).

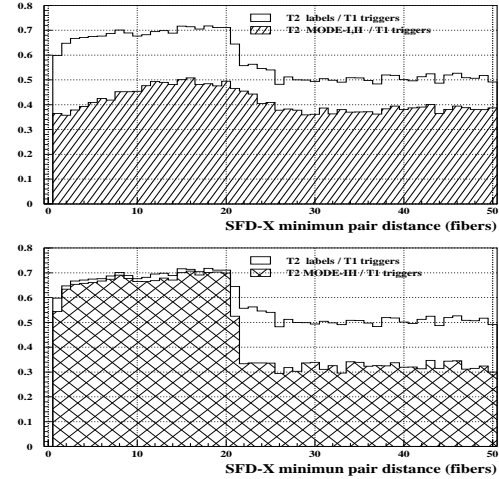


Figure 62: Top: ratio between  $T2$  MODE-(I+II) labels number and  $T1$  triggers number, function of SFD minimum pair  $x$ -distance. Bottom: ratio  $T2$  MODE-III/ $T1$  (time constrain 2 ns).

The most remarkable from the previous figures is how the background over 20 fibers increase in MODE-III when the time constrain is strong and we accept in our analysis

only hits with small time difference.

## 7 Conclusions

The previous analysis shows once more the complexity and difficulties of T2 trigger to select pairs with small  $x$  distance and minimum background contamination. The high multiplicity and the use of DE/DX and SFD information in a non strict combined way decrease the rejection factor of this trigger. To make a brief summary the following items could be useful:

- - The trigger rate of MODE-I and MODE-II is lower than the trigger rate for MODE-III and this is not what can be expected.
- - A loss of efficiency was detected for the detection of pairs with distance  $< 9\text{ mm}$  in run-III period with respect to run-II period.
- MODE-I and also MODE-II show an important background contamination at relative distances between hit-pairs  $> 9\text{ mm}$  when only the DE/DX detector produces a T2 trigger (T2-type 1, T2-type 2, T2-type 3). However MODE-I is the unique mode what is able to save the pairs that hit only one fiber.
- MODE-III establishes a clear cut at  $9\text{ mm}$ , but type-4 trigger is quite sensitive to high multiplicity in SFD detector and selects events that have low ionization signal.